IOP Conference Series: Materials Science and Engineering

PAPER • **OPEN ACCESS**

Visualizing the ion density distribution around a condensed phosphate phase at air-solid interface

To cite this article: Y Wang *et al* 2019 *IOP Conf. Ser.: Mater. Sci. Eng.* **479** 012082

View the article online for updates and enhancements.

This content was downloaded from IP address 107.150.122.145 on 15/10/2019 at 23:04

Visualizing the ion density distribution around a condensed phosphate phase at air-solid interface

Y Wang[1, 2, 3], Y Li[1], R L Liu[1], L Liu[2], L Xu[1], S Zhao[1] and H Bai[1]

[1] School of Medicine, Xi'an Peihua University, Xi'an, 710125, P. R. China;
[2] Shaanxi Key Laboratory of Degradable Biomedical Materials, School of Chemical Engineering, Northwest University, Xi'an, 710069, P. R. China.

[3] E-mail: lanmao1998@163.com; wangya1@peihua.cn

Abstract. The ion density distribution plays central roles in many interfacial phenomena and phase-transformation processes，which indirectly influences the formation, morphology and physical (or chemical) properties of the target matters. In this work, we report a simple method to visualize the ion density distribution of phosphate around a condensed phosphate phase during its formation at the air-solid interface.

1. Introduction

The density distribution of ions in the vicinity of interfaces has been a fundamental interest over the past decades, which could play important roles in many disciplines such as colloidal science, electrochemistry, surface science, heterogeneous catalysis and biology [1-9]. The conventional studies focus more attentions on the ion distribution near an interface such as the classical electrostatic double layer (EDL) theories. The theory is that the interface first develops charges by preferential adsorption and then is neutralized by an accumulation of dissolved counterions near the interface. The distribution of the counterions is described as EDL which has been well demonstrated in the most famous Gouy-Chapman-Stern (GCS) model [10-12]. The GCS model assumes that a typical EDL includes a dense monolayer of counterions (called Stern layer) adsorbed onto the interface and a diffuse layer of counterions whose density decays exponentially when moving away from the interface. However, a reliable picture of the ion density distribution of the EDL has remained elusive because of a lack of visualization methods. Although atomic force microscope (AFM) has been able to allows for imaging solid-liquid interfaces at 'true' atomic resolution [13–17], it seems to be only useful to detect Stern layer which is firmly bonded with the interface. As for the diffuse layer, it is difficult to be directly imaged by AFM because the ions distribution in this layer is quite easily perturbed. Additionally, the classical EDL theories are based on interfacial charge and only applicable to describe the ion density distribution within the nanometer-scale range near the interface. They are unable to help explain the ion distribution around a growing interface during liquid-to-solid phase transitions which may involve a large range of ion enrichment. In fact, the ion distribution is greatly important to understand the nucleation and the transient phases during new phase formation (especially for crystallization).

In this study, we developed a simple method to directly visualize the ion density distribution. First, an ion-containing substrate was built with phosphate and bovine serum albumin (BSA), then coated with an Au film of thickness over >20 nm. Thereafter, the Au-coated substrate was placed under an appropriate RH (relative humidity) condition for water vapor adsorption leading to the formation of a

Content from this work may be used under the terms of the Creative Commons Attribution 3.0 licence. Any further distribution of this work must maintain attribution to the author(s) and the title of the work, journal citation and DOI.
Published under licence by IOP Publishing Ltd

water adlayer on the Au-coated substrate. As the result, the phosphate ions was able to diffuse through the Au coating film into the water adlayer forming new phases (as a polymer with molecular weight about 66000, BSA molecules is unable to diffuse through the Au film; please refer to our previous work [18] for more details on the formation of the phosphate phase). With this method, the ion diffusion-caused density fluctuation within the Au film can be directly imaged with AFM and scanning electron microscope (SEM).

2. Materials and methods

2.1. Preparation of the BSA-phosphate substrate

A phosphate-containing substrate was prepared first by referring to the following procedures: A mix of 75 mg BSA (purity >98%; Merck) and 15 mg of phosphate ($Na_2HPO_4 \cdot 12H_2O$) was added to 1 mL of deionized water. Then, a droplet of the mixed solution (～10 μL) was added onto a silicon wafer (or electrically conductive glass) and dried on a hot stage preheated to 55-60 ℃ for 1-2 h under ambient conditions. Thereafter, the dried substrate was coated with an Au film and then placed under an appropriate RH (typically 45-60%) at room temperature for adsorption of ambient water vapour and for further characterizations.

2.2. Au coating

The samples were placed in an ion sputtering equipment (KYKY SBC-12) for Au coating. The source gas was air, the sputtering target was gold and the vacuum was 6-10 Pa. The thickness (d) of Au coating can be calculated with the formula: $d = KIVt$, where K is sputtering constant; I is plasma jet; V is sputtering voltage; t is sputtering time. The typical parameters are as follows: $K=0.07$; $I \geqslant 15$ mA; V=1kV; t >120s.

2.3. AFM observations

A commercial AFM instrument (Dimension Icon, Bruker) was employed to image the sample. In tapping mode imaging, a probe cantilever with a normal spring constant of ~40 N/m and a resonant frequency of ~300 kHz (RTESP, Veeco) was used. All images were captured with a scan rate of 1 Hz (at room temperature).

2.4. SEM imaging

A commercial scanning electron microscope (Vega3, Tescan) was used to image the samples. For SEM imaging, a sample must be prepared on an electrically conductive medium such as an electrically conductive glass. During imaging, the accelerating voltage was set to 15-20 kV.

3. Results and discussions

Within a few days, the sample was traced with tapping-mode AFM. As a result, it was found that many droplet-like phosphate phases (DLPPs) occurred on the substrate surface. In the height image (Figure 1a, left), only DLPPs could be clearly observed whereas in the phase image (Figure 1a, right), there was an additional annular area around the DLPP (darker contrast) showing quite different contrast (brighter contrast). This fact indicated that the annular area did not represent any real condensed phase, but instead represented ion diffusion-caused density fluctuation near the DLPP.

Except AFM, SEM was also used to observe the DLPP, which usually offers two imaging modes, i.e. secondary electron (SE) mode and back scattering electron (BSE) mode. In the former, the signal depth was typically on the order of nanoscale, while in the latter the depth could reach micrometer scale. As a result, it was found in the SE image (Figure 1b, left) that there was also an annular area around the individual DLPP. This evidence, along with the AFM result, verified the existence of annular area. Obviously, the occurrence of annular area should be due to the density fluctuation of phosphate ions within the Au coating. However, when observed with BSE mode (Figure 1b, right), the annular area could not be observed any more, suggesting that the ion diffusion behavior was mainly

active in the superficial layer of the substrate. To be specific, the ion density fluctuation probably took place in Au coating.

Here the visualization mechanism of ion density distribution is discussed (as shown in Figure 2). When the phosphate ions diffuse through the gaps of Au coating film and form DLPPs, the gaps near the DLPP will be also filled with enriched ions to meet the growth need of the DLPP. Once the ions are unevenly distributed around the DLPP, the physical or chemical properties of the corresponding annular area will be different from the further surrounding areas. The differences not only influence the tip-sample interactions in AFM imaging (phase signal), but also influence the electrical conductivity in SEM imaging (SE signal). As the result, the non-uniform ion density distribution can be detected out with the both methods.

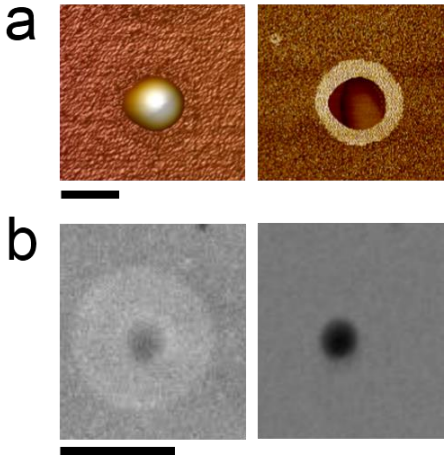


Figure 1. (a) Height (left) and phase (right) modes of AFM images of the DLPP, respectively. **(b)** SE (left) and BSE (right) modes of SEM images, respectively. Scale bars for all: 1 μm.

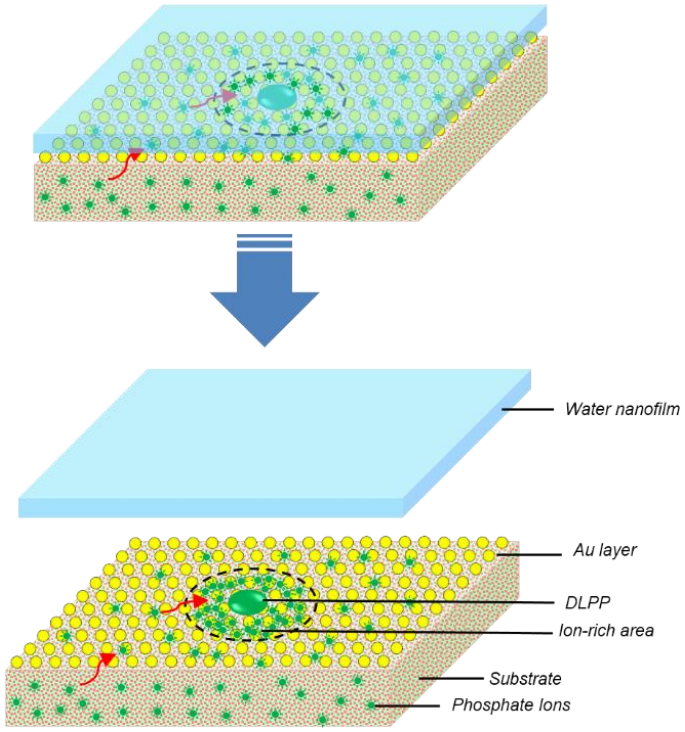


Figure 2. A schematic showing that the diffusion of phosphate ions through the Au coating and the formation of the ion-rich area around the DLPP.

4. Summary

In conclusion, we developed a novel and simple method to visualize the ion density distribution around a growing condensed phase. The results may contain a supplementary information to the current ion distribution theories and should be useful to expand the understandings on many disciplines such as colloidal science, electrochemistry, surface science and crystal growth.

Acknowledgements

The work was financially supported by the Scientific Research Starting Foundation of Xi'an Peihua University; the National Natural Science Foundation of China (21277210, 21476182); the National High Technology Research and Development Program of China (2014AA02108); the Scientific Research Program of Shaanxi Provincial Department of Education (12JK0449, 14JS102) and the NWU Graduate Innovation and Creativity Funds (YZZ14006).

References

[1] Ricci M, Spijker P and Voïtchovsky K 2014 *Nat. Commun.* **5** 4400
[2] Hugelmann M, Hugelmann P, Lorenz W and Schindler W 2005 *Surf. Sci.* **597** 156-72
[3] Lyklema J 2005 *Fundamentals of Interface and Colloid Science* (London: Elsevier)
[4] Bradshaw D, Garai A and Huo J 2012 *Chem. Soc. Rev.* **41** 2344-81
[5] Wandelt K and Thurgate S 2003 *Solid-liquid Interfaces: Macroscopic Phenomena, Microscopic Understanding* (Springer)
[6] Boström M, Williams D, Stewart P and Ninham B 2003 *Phys. Rev. E* **68** 041902
[7] Laanaita N, Mihaylova M, Hou B, Yu H, Vanýsek P, Meron M, Linc B, Benjamin I and Schlossman M L 2012 *P. Natl. Acad. Sci.* **109** 20326-31
[8] Luo G, Malkova S, Yoon J, Schultz D G, Lin B, Meron M, Benjamin I, Vanýsek P and Schlossman M L 2006 *Science* **311** 216-8
[9] G. Luo, S. Malkova, J. Yoon, D. G. Schultz, B. Lin, M. Meron, I. Benjamin, P. Vanýsek and M. L. Schlossman, *J. Electroanal. Chem.*, 2006, **593**, 142-58
[10] Guoy A 1910 J. Phys. *Theor. Appl.* **9** 457-68
[11] Chapman D L1913 *Philos. Mag.* **25** 475-81
[12] Stern O 1924 *Z. Electrochem. Angew. P.* **30** 508
[13] Siretanu I, Ebeling D, Andersson M P, S Stipp S L, Philipse A, Cohen Stuart M, van den Ende D and Mugele F 2014 *Sci. Rep.* **4** 4956
[14] Fukuma T, Kobayashi K, Matsushige K and Yamada H 2005 *Appl. Phys. Lett.* **87** 034101
[15] Voı¨tchovsky K, Kuna J J, Contera S A, Tosatti E and Stellacci F 2010 *Nat.Nanotechnol.* **5** 401-5
[16] Loh S H and Jarvis S P 2010 *Langmuir* **26** 9176-8
[17] Rode S, Hölscher R, Sanna S, Klassen S, Kobayashi K, Yamada H, Schmidt W G and Kühnle A 2012 *Phys. Rev. B* **86** 075468
[18] Wang Y, Fu R, Duan Z, Jiang X, Zhu C and Fan D 2018 *Chem. Commun.* **54** 9973-6